Egyptian Journal of Chemistry

http://ejchem.journals.ekb.eg/

Cerium organic frameworks as green pollution preventing materials for dye removal

Eman S. Mansor [1] and Tarek Aysha [2]

[1] *Water Pollution Research Department, Environmental Research and Climate Change Institute, National Research Centre, 33 El-Buhouth St., Dokki, Giza, Egypt. Postal code: 12622.*

[2] *Dyeing, Printing and Textile Auxiliaries Department, Textile Research and Technology Institute, National Research Centre, 33 EL Buhouth St., Dokki, Giza, 12622, Egypt*

Abstract

Cerium organic frameworks are presented in this work as pollutant preventing materials for the removal of reactive red 195 dye (RR 195) from aqueous solutions. Anthranilic acid and *β*-diketone as ligand sources were used in the separate state for the preparation of the cerium complexes metal organic frameworks (MOF1-MOF2) with a stoichiometric ratio 1:2 The prepared MOFs were used as adsorbent materials for decontamination of coloured solutions. The prepared materials were fully characterized by SEM, EDX, FTIR, surface area and zeta potential. The adsorption conditions (adsorption time, adsorbent loading, pH and dye concentration) were thoroughly optimized. The maximum adsorption capacity of the tertiary complex was more than that of the binary complexes. Different isothermal models (Langmuir, Freundlich, Temkin, and Dubinin–Kaganer–Radushkevich) have been studied. The physic-sorption adsorption of RR 195 behaviour is more fit to the Langmuir isotherm model through the pseudo-second-order kinetic model. That study introduces the promising cerium organic framework as pollution preventing material through dye removal.

Keywords: Diketone; anthranilic acid; metal organic frameworks; adsorption; anionic dyes.

1. Introduction

The usage of synthetic dyes has been widely introduced in numerous industries such as textile, leather tanning, rubber, and paper production [1-5]. Reactive dyes among the synthetic dyes are typically known in dyeing of different fabrics due to their ability to form a stable bond with the substrate by presenting a covalent bond between their active groups and the superficies groups of the fibers in the dyebath during dyeing process [6]. Otherwise, reactive dyes are the most hazardous dyes among the used colorants in textile applications. Reactive dyes especially azo dye category is one of the most type which is commonly used for dyeing of cellulosic fabrics as well as wool fabrics and very common as main colorants fraction which exist in dyeing and finishing manufactories wastewater. Recently textile wastewater includes refractory materials that cause critical environmental and health problems due to their persistent and non-biodegradability [7-16]. Different treatment strategies have been developed, including sedimentation, adsorption, coagulation-flocculation, reverse osmosis and anion exchange membranes for removal of colorants from the wastewater effluent [17-23].

The incomplete color removal by conventional techniques has been got attention, so colorants shall be expelled from the industrial waste water [24]

Adsorption has been made out to be an easy and fast technique in colorant removal due to its low cost, simple configuration and non-allergic to harmful substances. However its application is restricted by inefficiency activated carbon [25] mesoporous carbon [14], hydrotalcite [26], clay minerals [27], biopolymers [28], and agricultural by-products [29], biochar [30], EDTA modified Fe_3O_4/Sawdust carbon nanocomposites [31], and nanocomposite- MnO_2/BC [32].

Recently, newly adsorptive materials has been introduced for pollution control such as metal-

*Corresponding author e-mail: tarekaysha@hotmail.com; (Tarek Aysha).

Receive Date: 13 October 2022, **Revise Date:** 24 October 2022, **Accept Date:** 30 October 2022,
First Publish Date: 30 October 2022
DOI: 10.21608/EJCHEM.2022.168639.7084

organic frameworks (MOFs) or the development of inorganic-organic hybrid materials with a wide range of possible uses which is beside its efficient sorption capacity, can be used for drug delivery, photo-driven catalytic reactions, etc. [33, 34] MOFs have been applied for the elimination of many organic materials such as organic dyes [35], bisphenol [36], organic arsenic acids [37], pharmaceuticals / personal care products (PPPPs) and (2-Methyl – 4- chlorophenoxy) propionic acid (MCPP) from wastewater [38].

MOFs have attracted a lot of interest due to their high porosities. Moreover, MOFs have numerous conceivable applications including adsorption, separation of organic molecules and storage [39, 40]. MOFs have additionally been recognized as sorption and biosorption material for eliminating dangerous inorganic and organic pollutants, including adsorption of sulphur and nitrogen compounds [41, 42] and *E*. coli [43]. In addition, MOFs had been used as efficient material as antifungal and antibacterial [44] due to its stability resulted from the strong linkage between anthranilic acid and acetyl acetone, For the best of our knowledge, usage of binary and ternary cerium complexes for adsorptive removal of reactive red dye195 (RR 195) from water as adsorbent will be reported for the first time during this study to be used as green pollution preventive material as main goal of this study. Accordingly, the prepared cerium complexes were fully characterized and their adsorption capacity for removal of RR 195 anionic dye was evaluated. The adsorption process has been optimized and the adsorption behaviour has been demonstrated by studying different isothermal models and the adsorption kinetics.

2. Materials and methods

2.1. Materials

Cerium nitrate pentahydrate and anthranilic acid were purchased from Sigma Aldrich (purity > 99%). While, acetylacetone was obtained from Fluka (purity > 99%) and sodium hydroxide was purchased from (Sigma Aldrich, purity > 98%). Meanwhile, Hydrochloric acid (36%) was purchased from AcrosOrganics. The reactive dye (Synozol Red 6HBN, CI Reactive red 195 as shown in Fig.1) was purchased from KISCO South Korea

2.2. Methods

2.2.1. Synthesis of Schiff-base ligand (H_2L) 2-((4-oxopentan-2-ylidene)amino)benzoic acid

2-aminobenzoic acid (anthranilic acid) (0.02 mole, 2.74 g), acetylacetone (0.02 mole, 2g) were refluxed in ethanol 50 mL in presence of 2-3 drop of acetic acid as catalytic reagent for 4 h, then the mixture was concentrated by evaporation of ethanol using rotary evaporator and the formed yellow crystal was filtrated and washed with water. The obtained yield 66% and melting point 146-148 °C.

^{1}H-NMR (400 MHz, δ ppm, from TMS in $CDCl_3$) 12.95 (s, 1H, OH), 6.62–8.05 (m, 4H, ring proton), 5.25 (s, 1H, –CH=C-), 1.68 (s, 3H, CH_3), and 1.27 (s, 3H, CH_3). ^{13}C-NMR (400 MHz, δ ppm, from TMS in $CDCl_3$) 20.58, 24.96, 99.92, 116.31, 124.67, 126.27, 133.09, 135.45, 151.14, 160.89, 169.50, and 198.65. MS (m/z) 219.9 $[M]^+$. Elemental Anal. (%) Calcd C (65.75), H (5.93), and N (6.39). Found C (65.92), H (5.90), and N (6.53). FT-IR (KBr pellets, cm^{-1}) 1160 (C–O), 1213 (C–O), 1600 (C=N), and 3415 (O–H).

2.2.2. Preparation of binary Ce complex (MOF1)

Anthranilic acid (0.02mole, 2.74 g) was dissolved in 50 mL ethanol, $Ce(NO_3)_3{\cdot}6H_2O$ (0.01 mole, 3.26 g) was dissolved in 40 mL distilled water and the solution was added dropwise to anthranilic solution. The mixture was reflux for 2 h while the pH was adjusted at 8.0 by 0.2 M NaOH solution. The dark precipitate was then filtered, and the formed precipitate was filtrated and washed with distilled water. The obtained yield 72% and melting point >300 °C.

^{1}H-NMR (400 MHz, δ ppm, from TMS in DMSO-d^6) 6.91-7.89 (m, 8H, aromatic proton), 5.2 (s, 2H, NH proton). ^{13}C-NMR (400 MHz, δ ppm, from TMS in DMSO-d^6) 108.3, 117.2, 119.6, 132.4, 134.9, 148.5 and169.15. MS (m/z) 409.97 (100.0%), 410.93 (15.1%) $[M]^+$. Elemental Anal. (%) Calcd C (40.98), H (2.46), and N (6.38). Found C (41.01), H (2.45), and N (6.34). FT-IR (KBr pellets, cm^{-1}): 1389.45 (C–O), 1513 (C–O), 1615 (C=O), and 3420.1 (N–H).

Preparation of ternary Ce complex (MOF-2)

The ternary complex (MOF-2) was prepared by using the pervious prepared ligands H_2L. (0.02mole, 4.9 g) and 100 mL ethanol. Then, the aqueous solution of the (0.01mole, 3.26 g) $Ce(NO_3)_3{\cdot}6H_2O$ was added slowly to the previous mixture solution with adjusting pH at 8.0 by 0.2 M NaOH solution and the mixture was refluxed for 2h. The resulting reddish precipitate was then collected, washed with distilled water then dried. The obtained yield 61% and melting point >300°C.

^{1}H-NMR (400 MHz, δ ppm, from TMS in DMSO-d^6) 7.51-8.27 (m, 8H, aromatic proton), 5.2 (s, 1H, –CH=C-), 1.75 (s, 6H, $2CH_3$), 1.29 (s, 6H, $2CH_3$). ^{13}C-NMR (400 MHz, δ ppm, from TMS in DMSO-d^6) 18.9, 24.8, 90.8, 116.6, 125.1, 126.6, 128.5, 135.4, 149.7, 164.9, 174.6, 188. MS (m/z) 575.07 $[M]^+$. Elemental Anal. (%) Calcd C (50.17), H (3.86), and N (4.88). Found C (50.22), H (3.84),

and N (4.85). FT-IR (KBr pellets, cm^{-1}): 1039 (C-H), 1389 (C–O), 1531 (C=N), 1637 (C=O), 2923 C=C.

2.2.3. Characterization

Macro porous structures of the prepared materials were scanned using QUANTA FEG250 QUANTA FEG250 scanning electron microscopy (SEM) attached with Energy-dispersive X-ray spectroscopy (EDX) unit, using an accelerating voltage of 300 kV. The FTIR spectrum of the prepared materials was carried out on JASCO FTIR spectroscopy model 6100. Also the surface charge was determined by Particle Sizing Systems, Inc. Santa Barbara, Calif., USA. While, Quantachrome Touch Win™ was used for measuring Brunauer–Emmett–Teller (BET) surface area for the prepared materials.

2.2.4. Batch adsorption experimental

Batch experiments were carried out in a 100 mL conical flask to evaluate various parameters such as amount of adsorbent, pH, contact time, initial dye concentration. First the adsorbent amount experiments at different time intervals for 2 h were performed by mixing 50 mL solution of RR195 (50mgL^{-1}) initial dye concentration - pH 6.5)with various adsorbent amount from 0.5 gL^{-1} to 1.5 gL^{-1}.

The pH experiments were performed by using the optimum adsorbent amount and the pH values of the dye solutions were adjusted in the range of 3–11 using 0.1 M HCl and 0.1 M NaOH solutions. Then the effect of the dye concentrations on the removal of RR-195 dye by the prepared adsorbent were studied using different dye concentrations (40-80 mgL^{-1}) and the dye solutions were adjusted to pH3. All samples were automatically shaken at 150 rpm for 2h. From the initial time intervals to the equilibrium time the adsorbent was separated by centrifugation at 5000 rpm for 5 min.

The dye concentration was determined by measuring the absorbance value at λ_{max} = 535 nm using Carry 100 UV/Vis spectrophotometer. The dye uptake(q_t) (mgg^{-1}) at time t (min) calculated from the difference between the concentrations of RR195 before and after sorption using Equation 1and the adsorption capacity (q_e) (mgg^{-1}) at equilibrium were calculated using Equation 2: [45]

$$q_t = \frac{(C_0 - C_t)V}{m} \quad (1)$$

$$qe = \frac{(C_0 - C_e)V}{m} \quad (2)$$

Where, C_0, C_t and C_e (mgL^{-1}) were the dye concentrations at the initial, any time t, and at equilibrium in the solution, respectively. V (L) was the volume of the dye solution and m (g) was the mass of adsorbent. C_t was calculated by comparing the characteristic absorbance of dyes before and at time t after adsorption. C_e was the dye concentration at the equilibrium time. The calculation method was also applied to the adsorption kinetics as well as the adsorption isotherms. Two adsorption kinetic models, namely pseudo-first-order and pseudo-second-order, were used to evaluate the rate of adsorption of ternary cerium complex at five different concentrations. To determine the adsorption isotherms, Langmuir, Freundlich, Temkin and Dubinin–Kaganer–Radushkevich (DKR) isotherms models were explored to study the adsorption mechanism and to obtain the theoretical maximum adsorption capacity.

2.2.5. Adsorption using real textile wastewater

Sample was collected through a day using dosing pump of 250 mL.h^{-1}in order to represent the situation in the textile factories. The wastewater sample was collected from dyeing & finishing factory at El-Obour Industrial City located at the east of Cairo. The raw textile wastewater sample was characterized by determining the colour, turbidity, pH, Chemical Oxygen Demand (COD) and Biochemical Oxygen Demand (BOD_5) according to the Standard Methods for the Examination of Water and Wastewater, American Public Health Association (APHA), Washington, DC, USA. (2005). Adsorption experiments using the textile wastewater were proceeded by placing 250mL aliquots of the effluent. The samples were then centrifuged at 4000 rpm for 10 min. The initial and the final concentrations of colour and turbidity were measured as indicator for adsorption efficiency.

3. Results and discussion

3.1.1. Synthesis of H_2L ligand and MOFs

The Schiff base ligand (H_2L) was prepared by the same procedure as previously reported [46]. A direct condensation reaction between equal molar ratio of acetylacetone and anthranilic acid in mild acidic condition formed the Schiff base ligand (H_2L) in very good yield as shown in (scheme 1). The formed β-diketone ligand H_2L characterized by its keton-enol isomerization in weak acidic conditions. The synthesis of two new MOFs 1 and 2 as presented in scheme 1 was easy prepared due to the high reactivity of β-diketone ligand which binding easily with cerium nitrate salt forming 2:1 complex.

3.1.2. Characterization of cerium complexes

The prepared MOFs, using anthranilic acid as well as β-diketone ligand H_2L that are identified as MOF1 and MOF2 respectively, has been characterized to study their morphology, surface area, etc…

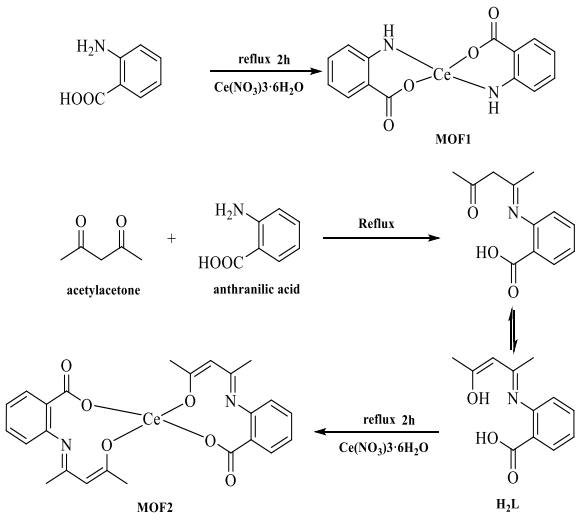

Scheme 1: the synthetic procedure of Schiff base ligand and its corresponding MOFs

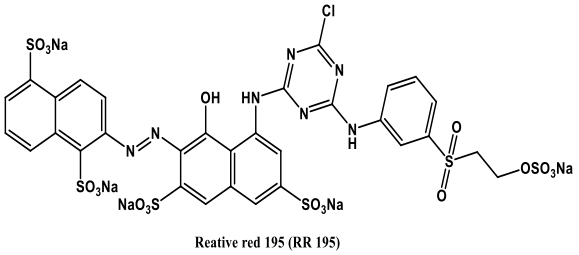

Fig. 1 the chemical structure of the commercial anionic dye (RR 195)

The morphology of the prepared MOFs has been demonstrated by SEM (Fig. 2). SEM images have been proved a difference in the microstructures of MOF1, MOF2 in Figs 2a, 1b respectively. The irregular shape of all the prepared materials and the boost in the permeable surface with the ternary complex as well as the pores on its surface will assist in understanding the adsorption procedure [47]. The SEM image of MOF2 showing irregular pores shape which is clearer comparing with MOF1 at 100 KX magnification.

Energy-dispersive X-ray spectroscopy (EDX) is a diagnostic tool used for understanding the content of the materials [37]. In this study, EDX was used to indicate the chemical composition of the prepared MOFs. Fig. 2 demonstrated the atomic percentage of C, O and Ce as 26.88%, 56.86%, and 13.25% for MOF1 and 57%, 28.64%, and 14.84 % respectively for MOF2.The previously presented elemental contents confirm the molar equivalent of ligand and cerium for the prepared complex as 1: 2 proportions for the ligand and the cerium source yet the percent of carbon is distinctive in respect to the previously utilized ligand.

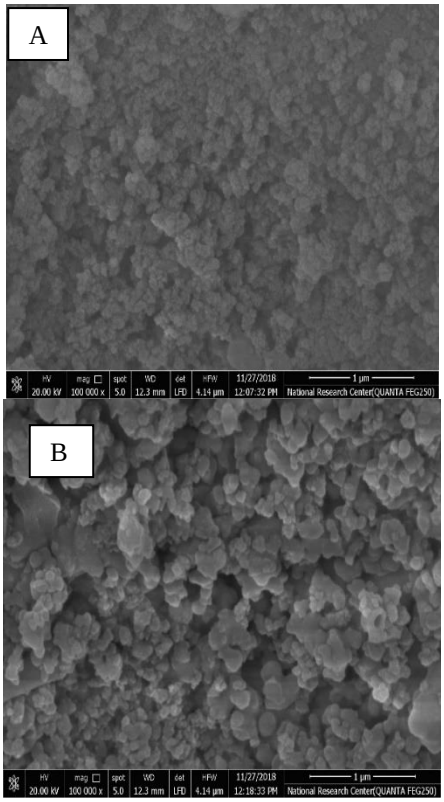

Fig. 2 SEM for the prepared cerium complexes MOF1 (A), MOF2 (B)

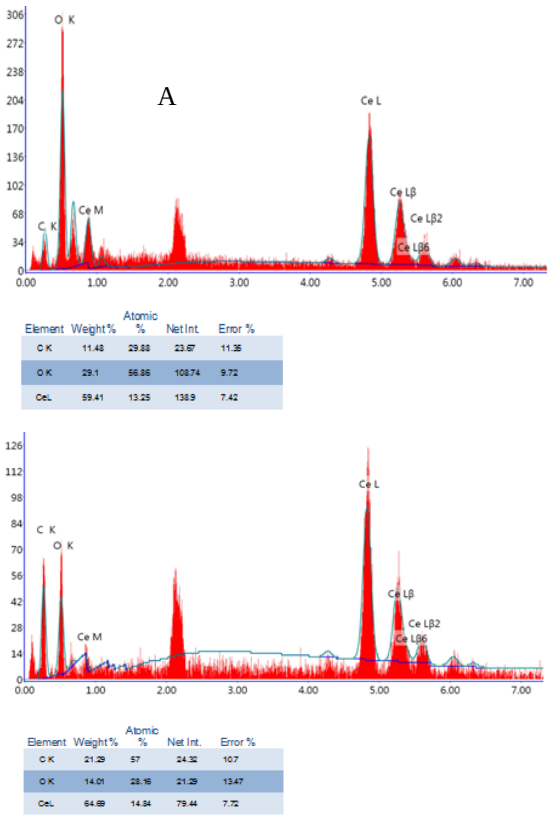

Fig. 3 Energy-dispersive X-ray spectroscopy (EDX) for the prepared cerium complexes (A) MOF1, (B) MOF2

The N_2 adsorption, isotherms and the surface area values of the studied materials has been demonstrated in Table 1. The ternary complex MOF2 has the highest recorded surface area comparing with MOF1. Likewise the Zeta potential properties values presented in the same table, the studied materials have positive charge at pH 7. Thus, at lower pH, RR 195 adsorption on ternary complex is expected to be ideal and appropriate.

Table 1. Adsorption, isotherms and the surface area values (BET) results at 77 K and surface charge for the prepared cerium complexes

	Isotherm		Adsorption		BET	
	Slope	Intercept	Correlation coeff., r	Constant	Surface area	Avg. Zeta Potential
MOF1	52.4543	1.01188	0.99986	52.8384	65.1349 m²/g	57.34 mV
MOF2	33.8915	0.149819	0.999244	227.216	102.303 m²/g	58.57 mV

The FTIR spectra of the prepared complexes were recorded with the extent of 400–4000 cm^{-1}. The data were listed and contrasted with each other to clarify the idea on the conceivable interactions for adsorbent-dye ion.

The scale in the range of 1200 and 1900 cm^{-1} is trademark for the vibrations of the β-diketon ligands. The FTIR range of the studied complexes indicates group series at 1612,1515, 1392 cm^{-1} [48]. These groups are indistinguishable to those announced for complexes and are ascribed to the vibrations of the carbonyl and the C-C double bonds in the conjugated chelate rings composed to the Ce^{+3} ion. In the hydroxyl region an expansive band around 3436 cm^{-1} is identified due to the hydrogen bonds between the surface OH groups and the β-diketon ligands [49]. The FTIR for MOF1, the crest at 3420 cm^{-1} is caused by amine group combination (–NH) or hydroxyl group (–OH). The tops at 1615 cm^{-1} were owed to the extending vibration of the carboxyl groups (–C=O). The bands at 1513 and 1389 cm^{-1}were ascribed to the extension of the carboxyl group vibration. The groups noticed at 1159 and 1035 cm^{-1} referred to alcoholic C-O and C-N extending vibration respectively, along these lines, the existence of hydroxyl and amine groups on the adsorbent surface was proved [50].

For the ternary complex formation (MOF2), the position of these bands is shifted toward lower side as compared to the free ligand and the binary complexes. The FTIR graph has good clear six characteristic peaks without any noises at 2923, 1637, 1531,1389 and 1039 cm^{-1}, which indicate the presence of -C-H, -C=O, -C=N and -C-N, respectively. That confirms the presence of the two started ligands within the final prepared material MOF2 and this coordination takes place through the nitrogen and oxygen atoms [44, 51] .

3.2. Optimizing adsorption parameters

Fig. 4 demonstrates the impact of different doses of the studied complexes (MOF1), (MOF2) for RR 195 removal. The adsorption of RR195 in presence of MOF1 and MOF2, has been significantly observed with the dose raise in MOF loads until the balance has been attained then desorption starts to take a place. Ideal load of the prepared materials was 1.25 g L^{-1}. With increment in the MOF1 and MOF2 portion, RR 195 adsorption was not considerable. Adsorption effectiveness of RR 195 in doses of 1.25 and 1.5 gL^{-1} were 89 and 90% individually for MOF1 and 95% for MOF2. The decolourization of the understudied dye with MOF1 and MOF2 portions can be owed to the high adsorbent surface and the accessibility of more adsorption sites [52]. With adsorbent loads >1.25 gL^{-1}, adsorption sites of MOFs has been covered ending with diminish altogether MOF's surface area [52, 53]. It is ascribed to the key component of adsorption capacity for the decolourization of the understudies dye in aqueous solutions is electrostatic attraction among MOFs and the function groups on the surface of the dye. Accordingly, Zeta potential is an adsorbent's significant factor that influences the interactions and the adsorption limit. As displayed above in Table 1 the zeta potential of MOF1 and MOF2 at pH 7 have high positive values, so these MOFs are a steady retentive toward anionic dyes solutions and should investigate the connection between pH of the dye solution and dye decolourization.

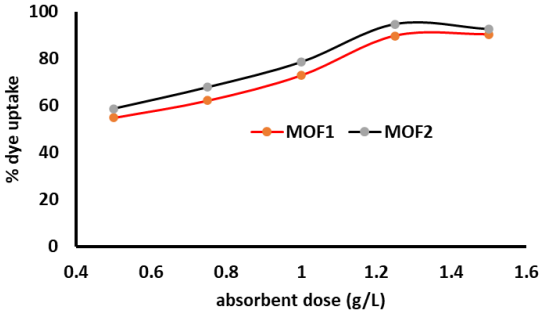

Fig.5 Effect of adsorbent dose (RR195 dye conc. 50mg/L; pH=6.5; reaction time=120min)

3.2.1. Effect of pH

pH is a standout amongst the most essential parameters that affect colour adsorption, due to the progress in the surface charges of the adsorbent and the level of ionization of the adsorbate [54], consequently the initial pH of the RR195 solution is

an important factor. In this study, RR 195 adsorption by the studied MOFs was investigated in different pH values in the range of (3 – 11) in order to assess the impact of pH on RR 195 adsorption. In this experiment0.125 g of MOF was added to 100 mL volume of RR 195 solution with starting concentration of 50 mgL^{-1}.

Fig.5 demonstrates RR 195 adsorption at different pH values. Boosting the pH from (3 – 11) significantly decrease the RR 195 adsorption in aqueous solution. The adsorption capacity of the anionic RR195 dye has been dropped steadily with increasing the pH values towards the alkaline medium and the significant drop has been recorded at pH 11 which is in accordance with Fikiru and Sahu 2018 [55],at pH< 7, positive surface charge has been expected due to high hydrogen ion concentration. At higher pH values, OH^- amount gradually incremented and RR 195 adsorption on MOF reduced due to repulsion force between the negative surface charge and the negative hydroxide ions[45, 56]. At pH 3, RR 195 adsorption on MOFs, most extreme adsorption was accomplished. Thus, pH 3 was chosen as optimum pH value for the following experiments to study the reaction kinetics.

The insets in Fig.5 apparently exhibit the colour variation of the MOFs after the colour adsorption. The huge pore size encourages the quick colour adsorption and this is coordinated with the SEM pictures for MOFs shown in Fig.2 that leads to conceivable co-adsorption of large RR 195 molecule. In addition, the appropriate pH_{PZC}, just as the generally large positive zeta potentials, clarify the capacity of MOFs to pull in oppositely charged dyes.

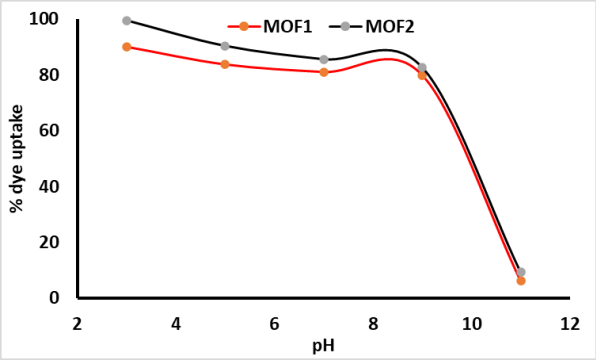

Fig. 5 The effect of pH on RR 195 adsorption onto cerium complexes at [dye conc.=50mg/L; dose 1.25 g/L; reaction time=60min.

3.3. Adsorption kinetics

In order to evaluate the effect of different RR 195 concentration, 40–80 $mgL^{-1}$of aqueous dye solutions were used at optimum contact time of 60 min.

Fig.6 shows the effect of RR 195 dye concentration on adsorption by MOFs. With increasing RR 195 concentration, adsorption efficiency decreased. Meanwhile in the case of MOF1,2 with dye concentration of 40 mgL^{-1}, RR 195 dye was completely adsorbed after 50 min due to adsorption of dye particles on MOFs adsorbent surface. While, incomplete removal has been recorded in higher concentrations due to the dissonance among RR 195 particles [57, 58].

MOF2 was selected to study the adsorption kinetics toward RR 195 dye solution which depicts the rate of solute take-up contingent upon the adsorption contact time.

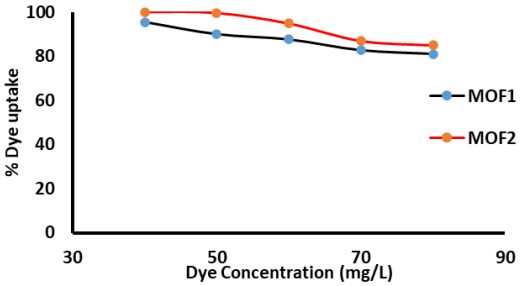

Fig.6 dye concentration effect on the efficiency in removal of RR-195 dye using the synthesized MOFs [Dose 1.25 g/L; pH 3 reaction time=90min]

The pseudo-first order model was firstly introduced where k_1 is the adsorption rate constant and determine from Equation 3.The integrated equation is shown by Equation 4. [59]

$$\boldsymbol{dq_t/d_t = k_1(q_e - q_t)} \qquad (3)$$

$$\boldsymbol{\ln(q_e - q_t) = \ln q_e - k_1 t} \qquad (4)$$

The quantity of dye adsorbed at time t before equilibrium represented by (q_t) while (q_e) represent the amount of the adsorbed dye at equilibrium. By plotting $\ln(q_e - q_t)$versus time (t), the rate constant is calculated from the slope. The correlation coefficients (R^2) were detected in the range of 0.9384-0.9709. Also, the experimental $q_e$vary from the determined ones as recorded in Table 2. Accordingly, the model of the pseudo-first order kinetic may not a substantial for clarification the RR-195 dye adsorption procedure onto MOF2 adsorbent. Kinetic model for pseudo-second-order is introduced by the next Equation 5.

$$\boldsymbol{t/q_t = \frac{1}{k_2 q_e^2} + t/q_e} \qquad (5)$$

Where, the rate constant of the second-order (g/mg min) is $k_2$that calculated for several concentrations relative to the direct plots of t/q_t versus time. It is obvious from Table 2 that the correlation coefficients R^2 were set in the highest range of 0.9667 - 0.9877.

It might be clarified that the pseudo-first - order model does not fit well to the entire range of contact time and generally under estimate the q_e values. The R^2 values for the pseudo second-order

model, on the other hand, were relatively larger than those for the pseudo first-order type. Accordingly, pseudo-second order kinetic was more appropriate for depicting the uptake of RR- 195 dye by MOF2 adsorbent.

Table 2. Models and parameters for adsorption kinetics using MOF2 for removal of RR-195 dye using

C_o (mg/L)	Q_e(mg/g)	Pesudo first order model		pesudo second order model	
		K_1(min^{-1})	R^2	K_2(g/mg min)	R^2
40	31.992	0.0215	0.9384	0.004223	0.9877
50	40.32	0.0161	0.9509	0.001955	0.9772
60	47.2	0.0127	0.9493	0.001584	0.9697
70	53.6	0.0126	0.9564	0.001705	0.9802
80	59.2	0.0114	0.9709	0.001117	0.9667

The model to get a better adsorption process is performed by the intraparticle diffusion and included two central steps through the movement of solute particles from the aqueous phase to the superficies of adsorbent which is followed by spread of the dye particles into the internal channels of the adsorbent. In general for adsorption system and correspond to this model, the quantity of adsorption is relative to $t^{1/2}$instead of t contact time and for this situation the adsorption rate can be all around assessed utilizing $t^{1/2}$ (half adsorption time) which is shown by Equation 6 [60].

$$\boldsymbol{q_t = k_{id}\, t^{1/2} + C} \qquad (6)$$

Where, k_{id} is rate constant of the intraparticle diffusion (mg.g^{-1}min$^{-1/2}$) and C (mg.g^{-1}) is the intercept. The intraparticle diffusion is expected by plotting the quantity of dye adsorbed (q_t) versus the square root of time at various beginning dye concentrations ($t^{1/2}$). The rate constant of the intraparticle diffusion (k_{id}) can be evaluated from their slope. The recognized values q_t were observed to be directly related to the $t^{1/2}$ and the intercept C values showed in Table 3gave data about the boundary layer thickness whereas strength to the direct relation between the outside mass exchange and the particle movement. The C constant incremented with raising RR-195 dye concentration and that trend was assigned to the thickness increase of the boundary layer.

The recorded R^2 values in Table 3 prove that the intraparticle diffusion model is the rate-limiting stage and the plots linearity show that the process of intraparticle diffusion had a noteworthy impact in the adsorption of dye RR-195 by MOF 2 adsorbent in aqueous solution.

The Elovich model is substantial for processes with heterogeneous superficies and it is reasonable and appropriate for chemisorption. The direct Elovich model is given by Equation 7 [59].

$$\boldsymbol{q_t = \frac{1}{\beta}\ln\alpha\beta + \frac{1}{\beta}\ln t} \qquad (7)$$

Where,α is the initial adsorption rate (mg g^{-1}.min) and β is identified with the degree of surface inclusion and the activation energy for chemisorption. A plot of q_t against *ln* t allows linearity with a slope of ($1/\beta$) and an intercept with $1/\beta\ln\alpha\beta$. The correlation coefficient recorded in Table 3 proved that the adsorption of RR-195 dye onto MOF2 adsorbent followed the pseudo second order kinetics.

Table 3. The intraparticle diffusion model and Elovich model for removal of RR-195A dye onto MOF2 adsorbent

C_o (mg/L)	Intra particle diffusion model		Elovich model		
	k_{id} (mg/g min$^{1/2}$)	R^2	α (mg/g min)	B (mg/g)	R^2
40	2.575	0.9662	3.9	0.146563	0.9898
50	3.556	0.9645	4.19	0.088496	0.9918
60	3.682	0.9836	4.6	0.086881	0.9936
70	4.039	0.9961	8	0.082372	0.9888
80	5.075	0.9952	5.5	0.063735	0.9942

3.4. Adsorption isotherms

The isotherm of adsorption is a critical methodology for the performance of how the adsorbent will interface and tie with the adsorbate. Moreover, adsorption models give a clue of the adsorption limit and assume an essential impact in concluding the conceivable adsorption process.

In this work Four different models have been introduced including Freundlich, Langmuir, Dubinin–Radushkevich (D–R) and Temkin isotherms [61].

The conveniently of these models is commonly discussed and assessed based on the correlation coefficient R^2. The Langmuir isotherm depends on the supposition that the adsorption procedure is supposed as a sort of chemical interaction in unimolecular shape [62]. The model is expressed by the linear Equation 8.

$$\boldsymbol{C_e/q_e = (1/q_{max})\, b + (C_e/q_{max})} \qquad (8)$$

Where C_e is the equilibrium concentration (mg.L^{-1}), qe is the amount of adsorbed dye (mg.g^{-1}) at equilibrium, and q max (mg.g^{-1}) and b (L.mg^{-1}) are the Langmuir constants associated with the adsorption limit and adsorption energy, respectively. The direct plot of C_e/q_e vs C_e (Fig. 7) shows a straight line with R^2 equal to 0.9992, indicating that adsorption follows the Langmuir isotherm model with monolayer adsorption of the understudied dye

with MOF2. The slope and intercept of the linear plot were used to obtain the values for B and q_{max} were derived from the linear plot's slope and intercept, where slope = $(1/q_{max})$ and the intercept= $(1/q_{max})\,b$. The fundamental attributes of Langmuir isotherm can be determined as far as dimensionless separation factor of the equilibrium parameter (R_L), which is calculated by Equation 9.

$$\boldsymbol{R_L = \frac{1}{1 + bC_0}} \qquad (9)$$

Where, C_0 is the essential concentration ($mg.L^{-1}$) of the adsorbate dye in the solution and b is the Langmuir constant connected to the adsorption energy ($L.mg^{-1}$). The determined R_L value indicate that the isotherm sort is positive ($0 < RL < 1$). R_L values were detected in the range of 0.002791-0.001397 referring to ideal MOF2 adsorbent for anionic dye removal.

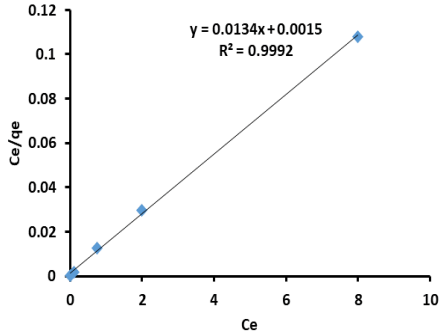

Fig. 7. Langmuir isotherm plot for adsorption of RR-195 onto MOF2 adsorbent

The Freundlich adsorption isotherm model [63] proposes a heterogeneous adsorption superficies with irregular accessible sites and varying adsorption energies. Freundlich's isotherm model is described by Equation 10.

$$\boldsymbol{q_e = K_F C_e^{1/2}} \qquad (10)$$

Where, qe is the quantity of adsorbed solute that is regarded to solute concentration at equilibrium C_e. The linear type of Freundlich isotherm is shown by Equation 11.

$$\boldsymbol{\ln q_e = \ln K_F + \frac{1}{n} \ln C_e} \qquad (11)$$

Where K_F is a constant and is defined as the adsorption or distribution associated with the bonding energy. It explains how much dye is adsorbed on the adsorbent surface ($mg.g^{-1}$) in relation to the adsorption limit. A plot of ln q_e vs ln C_e revealed a straight line with a slope of (1/n) and an intercept of ln KF, from which the values of KF and n may be calculated, and the evaluated parameters are listed in Table 4.

A plot of ln q_e vs ln C_e showed a straight line with the slope assigns a determination of the adsorption strength or superficies heterogeneity. The determined 1/n value (0.0927) is around zero therefore the adsorption system gets more heterogeneous as presented in Fig.8. By usual comparing of the correlation coefficients (R^2 = 0.9234) for Freundlich isotherm versus that of Langmuir (R^2 = 0.9992) demonstrates that Langmuir delivered a superior fitting for the exploratory equilibrium adsorption data than Freundlich isotherm as recorded in Table 4 and monolayer adsorption has been proved in adsorption of the understudied anionic dye with MOF2.

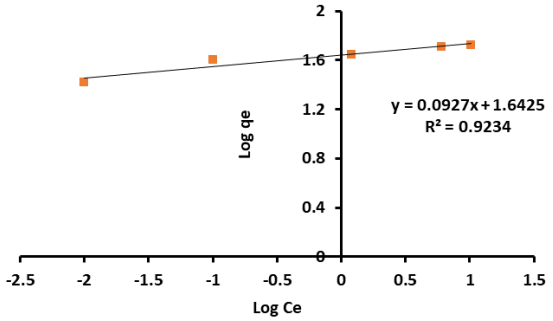

Fig.8 Freundlich model plot for adsorption of RR195 onto MOF2 adsorbent

The Temkin isotherm is depends on the statement that the heat of adsorption would diminish directly with the raise in adsorbent coverage. The straight type of this isotherm is represented by the next equations 12-14 [63].

$$\boldsymbol{q_e = \left(RT/b_T\right) \ln a_T + \left(RT/b_T\right) \ln C_e} \qquad (12)$$

$$\boldsymbol{q_e = B \ln a_t + B \ln C_e} \qquad (13)$$

$$\boldsymbol{B = \frac{RT}{b_T}} \qquad (14)$$

Where, q_e is the amount of the dye adsorbed at equilibrium; b_T (mgL^{-1}) is the constant of isotherm Temkin, a_T (Lg^{-1}) is constant at equilibrium binding constant. According to the graph of q_e vs ln C_e, The slope and intercept can be calculated, as well as the Temkin energy constants. B is a constant that is consistently associated with the adsorption heat ($J.mol^{-1}$) and their values are summarized in Table 4. The R^2 value which is distinguished as 0.9579 (Fig.9) may be used to verify a better connection of the Temkin isotherm.

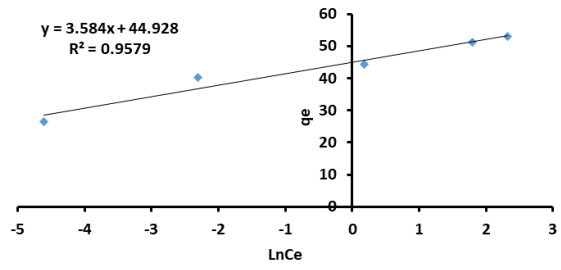

Fig. 9 Temkin isotherm, Adsorption isotherm models for RR 195 adsorption over MOF2

The Dubinin–Radushkevich (D–R) isotherm is often used to describe the mechanism of adsorption and to evaluate the porosity qualities of the adsorbent as well as the apparent energy of adsorption. Equation 15 estimates the direct equation of the D-R isotherm.[64].

$$\ln q_e = \ln q_e - (K_{ads}\varepsilon^2) \quad (15)$$

Where, qs is the hypothetical saturation limit ($mg.g^{-1}$), K_{ads} denotes the Dubinin-Radushkevich constant, which is associated with the mean free energy of adsorption per mole of adsorbate ($J.mol^{-1}$) and ε is the Polanyi potential, which is associated with equilibrium and denoted by Equation 16..

$$\varepsilon = RT\ln\left(1 + {}^{1}/_{C_e}\right) \quad (16)$$

R representing the gas constant value, T is the temperature in Kelvin. Plotting ln q_e vs ε^2, a straight line formed with a slope equal K_{ads} and intercept equal ln qs. The q_s ($mg.g^{-1}$) and K_{ads} ($mol^2.k^{-1}J^{2(-1)}$) values were determined and found 23 and 0.0004685, respectively. Meanwhile, the recognized R^2 is 0.945 which demonstrate acceptable fitting to this isotherm model as introduced in Fig.10. The consequences of this study is a monolayer physisoprtion behaviour has been confirmed for RR- 195 dye adsorption by MOF2 adsorbent.

3.5. Regeneration of MOF2 and reusability

The facile regeneration and reusability test of MOF2 is performed for possible implementation in the large scale. The prepared adsorbent MOF2 was regenerated with 0.1N HCl and the adsorption capacity of the regenerated MOF2 for eight cycles was investigated under optimized conditions as in previous and compared to the first cycle as shown in Fig. 11. The adsorption capacity of RR 195 onto MOF2 not decrease with increasing reusability cycles up to 8 cycles with slight decrease after the fourth cycle. After eight cycles, removal efficiency is still above 99%. So, MOF2 can be easily reused many times after regeneration, demonstrating that this adsorbent has a high potential for dye adsorption in wastewater.

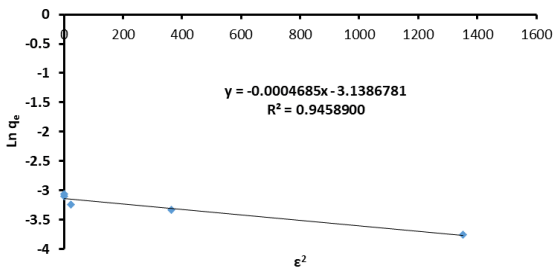

Fig.10 D-R isotherm adsorption isotherm models for RR 195 adsorption over MOF2

Table 4. Isotherm parameters of Langmuir, Freundlich, Temkin and D-R models

Adsorption model	Isotherm parameters	
langmuir	q_m (mg/g)	74.6
	b(L/mg)	8.9
	R_L	0.002791 - 0.001397
	R^2	0.9992
freundlich	1/n	0.235
	K_F (L/mg)	7.925
	R^2	0.931
temkin	a_T(L/g)	268227
	b_T	702.8
	B(J/mol)	3.584
	R^2	0.9579
D-R	q_s(mg/g)	23
	K_{ads} (mol^2/KJ^2)	0.0004685
	R^2	0.945

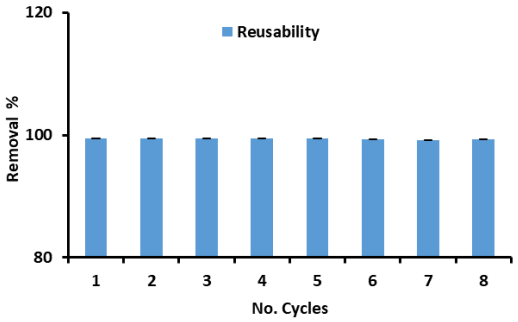

Fig. 11 the cycling index of the removal of RR 195 from regenerated MOF2 (Dye concentration: 50 mg/L; Dose: 1.25 g/L; pH 3)

3.6. Adsorption using real wastewater

MOF2 has been evaluated as an adsorbent to treat real wastewater sample from the collected textile industries, the evaluation includes dyes and different chemicals. The real wastewater sample from dyeing factory contains not only dyes but also different components such as auxiliaries and salts which can affect and interfere in the adsorption process.

Fig 12 shows that the BOD5/COD ratio was approximately 0.39 indicating only physicochemical treatment, or the combination of physicochemical. Because wastewater from the textile sector contains low levels of biodegradable organic compounds, these findings were expected. Thus, for textile wastewater, physicochemical treatment is usually sufficient, with no additional biological treatment required. [65].

In terms of the MOF2 adsorption trials with real wastewater, during 90 mints the colour of the sample was reduced from the initial absorbance 0.41 to 0.017 at λ_{max} 495 nm, which means the removal percentage of dye reach 95.9%.

The turbidity was decreased from 164 to 9 NTU following the adsorption procedure, representing an 84.7% reduction. Harrelk as et al. (2009) [66] Textile wastewater treatment was investigated using several physicochemical process combinations. Combining coagulation/ flocculation (CF) with adsorption on activated carbon (AC) resulted in a colour reduction of only 50%, which is less than that achieved in this study. While Bayramoglu et al. (2007) [67], investigated the effect of different aluminum and iron electrode configurations on the valuable removal of textile wastewater electrocoagulation treatment, achieving 83 and 80% turbidity removal using Fe and Al electrodes, respectively, which is less than that achieved in this study. These findings suggest that MOFs can be utilized to clean genuine textile effluent.

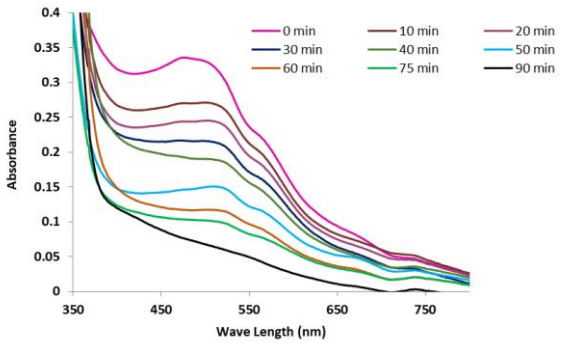

Fig. 12 real wastewater treatment using MOF2 (Dose: 1.25 g/L; pH 7.3)

Table 5 is a comparison of the adsorption capacity of some adsorbents reported previously for dye removal. Compared with other metal oxide-based adsorbents, MOF2 presented in this study has high capacity as presented [16, 32, 68]. Also by comparing with MOF Uio-66, it can be potentially an effective adsorbent for RR 195 [58]. However, there are other MOFs that have high adsorption capacity attributes to the highest condition for preparing these MOFs which is considered costly ineffective preparation methods [45, 69].

Table 5: wastewater properties before and after treatment using MOF2

Parameter	raw real wastewater	real wastewater after treatment
pH	7.3	7.3
Colour	0.41	0.017
Turbidity (NTU)	164	9
BOD5 (mg.L-1)	210	35
COD (mg.L-1)	550	85
TSS (mg.L-1)	84	16

4. Conclusion

Different cerium organic complexes have been prepared by using β diketon ligand. Semi-empirical calculations indicated that Metal (Cerium) organic frameworks (MOFs) can be applied as green solution for removing Reactive Red 195(RR) dye from aqueous solutions. The prepared β diketon ligand have been used as ligand source of the binary cerium complexes (MOF1- MOF2) as 1:2 stoichiometry complexes. These materials showed excellent adsorption behaviour because of their intrinsic porosity, organized channel structure, high surface area, stability, and functionality. These characteristics have been proved by SEM, EDX, FTIR, surface area and zeta potential beside the high removal rate of reactive red 195 dye. The adsorption conditions have been optimized to 1.25 g L^{-1} of MOFs for removal of 95% of 50 mg L^{-1} dye at pH3.

The results investigated that adsorption limits of ternary complex were much higher than of binary complex. The exploratory information could be better allowed by the Langmuir isotherm model and demonstrate the capacity of MOF2 to adsorb 74.6 mg of RR 195 for each gram of adsorbent at the ideal conditions. The coexistence of physisorption behaviour in this process, with intra-particle diffusion as a rate controlling step is following a pseudo-second-order kinetic model.

Acknowledgement

We are very grateful to Prof. Dr. Tarek Samir, National research Centre for his support and visualization of the manuscript idea, planning of work and editing of final form of the manuscript.

Declarations

Conflict of interest: The authors declare no competing interests.

References

[1] T. Aysha, M. Zain, M. Arief, Y. Youssef, Alkali-stable solid state fluorescent pyrazolo/pyrrolinone disperse dyes: Synthesis and application for dyeing polyester fabric, J Mol Struct 1249 (2022).

[2] T. Aysha, M. Zain, M. Arief, Y. Youssef, Synthesis and spectral properties of new fluorescent hydrazone disperse dyes and their dyeing application on polyester fabrics, Heliyon 5(8) (2019).

[3] T. Aysha, M. El-Sedik, H.M. Mashaly, M.A. El-Apasery, O. Machalicky, R. Hrdina, Synthesis, characterisation, and applications of isoindigo/pechmann dye heteroanalogue hybrid dyes on polyester fabric, Color Technol 131(4) (2015) 333-341.

[4] S. Lunak, T. Aysha, A. Lycka, O. Machalicky, R. Hrdina, Structure and absorption of co(iii) azo complex dyes based on pyrrolinone esters: Dft and td dft study, Chem Phys Lett 608 (2014) 213-218.
[5] M. Eldessouki, T. Aysha, M. Raticakova, J. Saskova, V.V.T. Padil, M. Ibrahim, M. Cernik, Structural parameters of functional membranes for integration in smart wearable materials, Fibres Text East Eur 25(5) (2017) 73-78.
[6] M. El-Sedik, S. Abd Elmegied, T. Aysha, S.A. Mahmoud, Synthesis and application of new reactive disperse dyes based on isatin derivatives and their antibacterial activity, Egypt J Chem 62(12) (2019) 2253-2264.
[7] K. Azam, N. Shezad, I. Shafiq, P. Akhter, F. Akhtar, F. Jamil, S. Shafique, Y.K. Park, M. Hussain, A review on activated carbon modifications for the treatment of wastewater containing anionic dyes, Chemosphere 306 (2022).
[8] S. Sehar, T. Rasool, H.M. Syed, M.A. Mir, I. Naz, A. Rehman, M.S. Shah, M.S. Akhter, Q. Mahmood, A. Younis, Recent advances in biodecolorization and biodegradation of environmental threatening textile finishing dyes, 3 Biotech 12(9) (2022).
[9] D. Selvaraj, N.K. Dhayabaran, A. Mahizhnan, An insight on pollutant removal mechanisms in phycoremediation of textile wastewater, Environ Sci Pollut R (2022).
[10] R.A. Mashabi, Z.A. Khan, K.Z. Elwakeel, Chitosan- or glycidyl methacrylate-based adsorbents for the removal of dyes from aqueous solutions: A review, Mater Adv 3(14) (2022) 5645-5671.
[11] E. Gayathiri, P. Prakash, K. Selvam, M.K. Awasthi, R. Gobinath, R.R. Karri, M.G. Ragunathan, J. Jayanthi, V. Mani, M.A. Poudineh, S.W. Chang, B. Ravindran, Plant microbe based remediation approaches in dye removal: A review, Bioengineered 13(3) (2022) 7798-7828.
[12] D. Vishnu, B. Dhandapani, S. Authilingam, S.V. Sivakumar, A comprehensive review of effective adsorbents used for the removal of dyes from wastewater, Curr Anal Chem 18(3) (2022) 255-268.
[13] A. Aguedach, S. Brosillon, J. Morvan, E.K. Lhadi, Photocatalytic degradation of azo-dyes reactive black 5 and reactive yellow 145 in water over a newly deposited titanium dioxide, Appl Catal B-Environ 57(1) (2005) 55-62.
[14] D.D. Asouhidou, K.S. Triantafyllidis, N.K. Lazaridis, K.A. Matis, S.S. Kim, T.J. Pinnavaia, Sorption of reactive dyes from aqueous solutions by ordered hexagonal and disordered mesoporous carbons, Micropor Mesopor Mat 117(1-2) (2009) 257-267.
[15] S. Rosa, M.C.M. Laranjeira, H.G. Riela, V.T. Favere, Cross-linked quaternary chitosan as an adsorbent for the removal of the reactive dye from aqueous solutions, J Hazard Mater 155(1-2) (2008) 253-260.
[16] V. Belessia, Romanosa,G., Boukosa,N. , Lambropouloud,D., Trapalis,C. , Removal of reactive red 195 from aqueous solutions by adsorption on the surface of tio2 nanoparticles, Journal of Hazardous Materials 170 (2009) 836-844.
[17] T. Robinson, G. McMullan, R. Marchant, P. Nigam, Remediation of dyes in textile effluent: A critical review on current treatment technologies with a proposed alternative, Bioresource Technol 77(3) (2001) 247-255.
[18] I.D. Mall, V.C. Srivastava, N.K. Agarwal, I.M. Mishra, Removal of congo red from aqueous solution by bagasse fly ash and activated carbon: Kinetic study and equilibrium isotherm analyses, Chemosphere 61(4) (2005) 492-501.
[19] Y.M. Slokar, A.M. Le Marechal, Methods of decoloration of textile wastewaters, Dyes Pigments 37(4) (1998) 335-356.
[20] H. El-Kholly, S. Abdel Moneim, H. Ibrahim, N. Ammar, A. El-Deen, M.H. Helal, M.K. Zahran, M. Ali, Surface decoration of zirconium oxide with bismuth sulfide catalysts for photocatalytic degradation of red dye 195, Egypt J Chem 65(10) (2022) 209-215.
[21] M.A. El-Apasery, A. Aly, D. Ahmed, Decolorization of reactive dyes, part v: Eco-friendly approach of reactive red 195 dye effluents decolorization using geopolymer cement based on metakaolin, Egypt J Chem 65(12) (2022) 121-127.
[22] M.A. El-Apasery, D. Ahmed, A. Aly, Decolorization of reactive dyes, part iv: Eco-friendly approach of reactive red 195 dye effluents decolorization using geopolymer cement based on slag, Egypt J Chem 65(12) (2022) 129-135.
[23] R. Al araby, M. El Sayed, Methylene blue cationic dye removal using aa-am hydrogel as an efficient adsorbent, Egypt J Chem 65(12) (2022) 1-10.
[24] M. Ahmed, M.O. Mavukkandy, A. Giwa, M. Elektorowicz, E. Katsou, O. Khelifi, V. Naddeo, S.W. Hasan, Recent developments in hazardous pollutants removal from wastewater and water reuse within a circular economy, Npj Clean Water 5(1) (2022).
[25] P.K. Malik, Dye removal from wastewater using activated carbon developed from sawdust:

Adsorption equilibrium and kinetics, J Hazard Mater 113(1-3) (2004) 81-88.
[26] N.K. Lazaridis, T.D. Karapantsios, D. Georgantas, Kinetic analysis for the removal of a reactive dye from aqueous solution onto hydrotalcite by adsorption, Water Res 37(12) (2003) 3023-3033.
[27] S.D. Lambert, N.J.D. Graham, C.J. Sollars, G.D. Fowler, Evaluation of inorganic adsorbents for the removal of problematic textile dyes and pesticides, Water Sci Technol 36(2-3) (1997) 173-180.
[28] M.S. Chiou, H.Y. Li, Equilibrium and kinetic modeling of adsorption of reactive dye on cross-linked chitosan beads, J Hazard Mater 93(2) (2002) 233-248.
[29] X.S. Wang, Y. Zhou, Y. Jiang, C. Sun, The removal of basic dyes from aqueous solutions using agricultural by-products, J Hazard Mater 157(2-3) (2008) 374-385.
[30] V. Bharti, K. Vikrant, M. Goswami, H. Tiwari, R.K. Sonwani, J. Lee, D.C.W. Tsang, K.H. Kim, M. Saeed, S. Kumar, B.N. Rai, B.S. Giri, R.S. Singh, Biodegradation of methylene blue dye in a batch and continuous mode using biochar as packing media, Environ Res 171 (2019) 356-364.
[31] N. Kataria, V.K. Garg, Application of edta modified fe3o4/sawdust carbon nanocomposites to ameliorate methylene blue and brilliant green dye laden water, Environ Res 172 (2019) 43-54.
[32] S.I.M. Siddiqui, O. Mohsin, M. Chaudhry, S. A., Nigella sativa seed based nanocomposite-mno2/bc: An antibacterial material for photocatalytic degradation, and adsorptive removal of methylene blue from water, Environ Res 171 (2018) 328-340.
[33] K. Ariga, A. Vinu, Y. Yamauchi, Q.M. Ji, J.P. Hill, Nanoarchitectonics for mesoporous materials, B Chem Soc Jpn 85(1) (2012) 1-32.
[34] A. Vinu, K. Ariga, New ideas for mesoporous materials, Adv Porous Mater 1(1) (2013) 63-71.
[35] S.H. Huo, X.P. Yan, Metal-organic framework mil-100(fe) for the adsorption of malachite green from aqueous solution, J Mater Chem 22(15) (2012) 7449-7455.
[36] M.M. Zhou, Y.N. Wu, J.L. Qiao, J. Zhang, A. McDonald, G.T. Li, F.T. Li, The removal of bisphenol a from aqueous solutions by mil-53(al) and mesostructured mil-53(al), J Colloid Interf Sci 405 (2013) 157-163.
[37] B.K. Jung, J.W. Jun, Z. Hasan, S.H. Jhung, Adsorptive removal of p-arsanilic acid from water using mesoporous zeolitic imidazolate framework-8, Chem Eng J 267 (2015) 9-15.
[38] Z. Hasan, E.J. Choi, S.H. Jhung, Adsorption of naproxen and clofibric acid over a metal-organic framework mil-101 functionalized with acidic and basic groups, Chem Eng J 219 (2013) 537-544.
[39] H. Furukawa, Cordova,K.E. , O'Keeffe,M. , Yaghi,O.M. , The chemistry and applications of metal-organic frameworks, , Science 341 (2013) 1230444.
[40] S.H. Jhung, Khan,N.A.,Hasan, Z. , Analogous porous metal-organic frameworks: Synthesis, stability and application in adsorption, Crystengcomm 14 (2012) 7099-7109.
[41] K.A. Cychosz, A.G. Wong-Foy, A.J. Matzger, Enabling cleaner fuels: Desulfurization by adsorption to microporous coordination polymers, J Am Chem Soc 131(40) (2009) 14538-14543.
[42] I. Ahmed, N.A. Khan, Z. Hasan, S.H. Jhung, Adsorptive denitrogenation of model fuels with porous metal-organic framework (mof) mil-101 impregnated with phosphotungstic acid: Effect of acid site inclusion, J Hazard Mater 250 (2013) 37-44.
[43] A. Gupta, S.K. Bhardwaj, A.L. Sharma, K.H. Kim, A. Deep, Development of an advanced electrochemical biosensing platform for e. Coli using hybrid metal-organic framework/polyaniline composite, Environ Res 171 (2019) 395-402.
[44] M.A.H. Md. Rabiul Hasan, Md. Abdus Salam,Mohammad Nasir Uddin, Nickel complexes of schiff bases derived from mono/diketone withanthranilic acid: Synthesis, characterization and microbial evaluation., Journal of Taibah University for Science 10 (2016) 766-773.
[45] H.C. Li, Xinyu Zhang, Chuang Yu, Qing Zhao, Zijian Niu, Xuedun Sun, Xiaodong Liu, Yunling Ma, Li Li, Zhengqiang, Enhanced adsorptive removal of anionic and cationic dyes from single or mixed dye solutions using mof pcn-222, Rsc Adv 7(27) (2017) 16273-16281.
[46] C.R. Bhattacharjee, P. Goswami, M. Sengupta, Synthesis, electrochemical and antimicrobial studies of mono and binuclear iron(iii) and oxovanadium(iv) complexes of [ono] donor tridentate schiff-base ligands, J Coord Chem 63(22) (2010) 3969-3980.
[47] K.Y.A. Lin, S.Y. Chen, A.P. Jochems, Zirconium-based metal organic frameworks: Highly selective adsorbents for removal of phosphate from water and urine, Mater Chem Phys 160 (2015) 168-176.
[48] Z.K. Muhammad Saeed, Rabia Saleem, Synthesis and chemical characterization of

metals (al, cr, co, mn and vo) complexes with acetylacetone (β-diketone), (2017).
[49] B.M. Wuckhysun, Synthesis, spectroscopy and catalysis of [cr $(acac)_3$] complexes grafted on to mcm-41 materials : Formation of polyethylene nanofiders within mesoporous crystaline aluminosilicates 6(2000) 2960-2970.
[50] T.S.J. Eman S. Mansor, Heba Abdallah, A.M. Shaban, Highly thin film nanocomposite membrane based metal organic complexes for brackish water desalination, Journal of Environmental Chemical Engineering 6 (2018) 5459-5469.
[51] P.R. Shirode , Patil,D.C., Synthesis and physicochemical studies of mixed ligand complexes of salicyladehyde anthranilic acid and salicyladehyde semicarbazone, 5 (2016) 20703-20708.
[52] A. Maleki, Daraei, H., Khodaei, F., Aghdam, K.B. and Faez, E., 2016. , Direct blue 71 dye emoval probing by potato peel-based sorbent: Applications of artificial intelligent systems., Desalination and Water Treatment 57 (2016) 12281-12286.
[53] M.T. Yagub, Sen, T.K., Afroze, S. and Ang, H.M. , Dye and its removal from aqueous solution by adsorption: A review. , Advances in colloid and interface science, 209 (2014) 172-.
[54] L.F. Guo H, Chen J, Li F, Weng W, , Metal-organic framework mil-125(ti) for efficient adsorptive removal of rhodamine b from aqueous solution, , Appl Organomet Chem 29 (2015) 12-19.
[55] N.G. Fikiru Temesgen , Omprakash Sahu, Biosorption of reactive red dye (rrd) on activated surface of banana and orange peels: Economical alternative for textile efßuent, Surfaces and Interfaces 12 (2018) 151-159.
[56] J.-J.W. Li, Chong-Chen Fu, Hui-fen Cui, Jing-Rui Xu, Peng Guo, Jie Li, Jian-Rong, High-performance adsorption and separation of anionic dyes in water using a chemically stable graphene-like metal–organic framework, Dalton Transactions 46(31) (2017) 10197-10201.
[57] E.R.M. Garcia, R. L. Lozano, M. M. Hernandez Perez, I. Valero, M. J. Franco, A. M. M., Adsorption of azo-dye orange ii from aqueous solutions using a metal-organic framework material: Iron- benzenetricarboxylate, Materials (Basel, Switzerland) 7(12) (2014) 8037-8057.
[58] A.A. Mohammadi, Alinejad,A.,Kamarehie, B. Javan,S., Ghaderpoury,A., Ahmadpour,M., Ghaderpoori,M., Metal-organic framework uio-66 for adsorption of methylene blue dye from aqueous solutions, Int. J. Environ. Sci. Technol 14(9) (2017) 9.
[59] M.E.N. Mahmoud, Gehan M. El-Mallah, Nabila M. Bassiouny, Heba I. Kumar, Sandeep Abdel-Fattah, Tarek M., Kinetics, isotherm, and thermodynamic studies of the adsorption of reactive red 195 a dye from water by modified switchgrass biochar adsorbent, Journal of Industrial and Engineering Chemistry 37 (2016) 156-167.
[60] K.V.K. Porkodi, K., Equilibrium, kinetics and mechanism modeling and simulation of basic and acid dyes sorption onto jute fiber carbon: Eosin yellow, malachite green and crystal violet single component systems, Journal of Hazardous Materials 143(1) (2007) 311-327.
[61] H.F.Y. Tarek S. Jamil Microwave synthesis of zeolites from egyptian kaolin: Evaluation of heavy metals removal, separation science and technology 51 (2016) 2876-2886.
[62] P.S. Kumar, Ramalingam, S., Senthamarai, C., Niranjanaa, M., Vijayalakshmi, P. and Sivanesan, S., Adsorption of dye from aqueous solution by cashew nut shell: Studies on equilibrium isotherm, kinetics and thermodynamics of interactions. , Desalination 261 (2010) 52-60.
[63] S.J.M. Allen, G. Porter, J. F., Adsorption isotherm models for basic dye adsorption by peat in single and binary component systems, J Colloid Interface Sci 280(2) (2004) 322-33.
[64] A.A. Gunay, E. Tosun, I., Lead removal from aqueous solution by natural and pretreated clinoptilolite: Adsorption equilibrium and kinetics, J Hazard Mater 146(1-2) (2007) 362-71.
[65] E. GilPavas, I. Dobrosz-Gomez, M.A. Gomez-Garcia, Coagulation-flocculation sequential with fenton or photo-fenton processes as an alternative for the industrial textile wastewater treatment, J Environ Manage 191 (2017) 189-197.
[66] F. Harrelkas, A. Azizi, A. Yaacoubi, A. Benhammou, M.N. Pons, Treatment of textile dye effluents using coagulation-flocculation coupled with membrane processes or adsorption on powdered activated carbon, Desalination 235(1-3) (2009) 330-339.
[67] M. Bayramoglu, M. Eyvaz, M. Kobya, Treatment of the textile wastewater by electrocoagulation economical evaluation, Chem Eng J 128(2-3) (2007) 155-161.
[68] X.Y. Jiajin Zhang, Mengqing Hu, Xiaoyan Hu, Min Zhou, Adsorption of congo red fromaqueous solution using zno-modified sio_2 nanospheres with rough surfaces, Journal of Molecular Liquids 249 (2018) 772–778.

[69] E.R. Garcia, R.L. Medina, M.M. Lozano, I.H. Perez, M.J. Valero, A.M.M. Franco, Adsorption of azo-dye orange ii from aqueous solutions using a metal-organic framework material: Iron-benzenetricarboxylate, Materials 7(12) (2014) 8037-8057.